DOE/NASA/51040-51
NASA TM-83539

Bending Fatigue of Electron-Beam-Welded Foils

Application to a Hydrodynamic Air Bearing in the Chrysler/DOE Upgraded Automotive Gas Turbine Engine

J. F. Saltsman and G. R. Halford
National Aeronautics and Space Administration
Lewis Research Center

January 1984

Prepared for
U.S. DEPARTMENT OF ENERGY
Conservation and Renewable Energy
Office of Vehicle and Engine R&D

DISCLAIMER

Printed in the United States of America

Available from
National Technical Information Service
U.S. Department of Commerce
5285 Port Royal Road
Springfield, VA 22161

NTIS price codes[1]
Printed copy: A02
Microfiche copy: A01

[1]Codes are used for pricing all publications. The code is determined by the number of pages in the publication. Information pertaining to the pricing codes can be found in the current issues of the following publications, which are generally available in most libraries: *Energy Research Abstracts (ERA); Government Reports Announcements* and Index (*GRA* and I); *Scientific and Technical Abstract Reports (STAR);* and publication, NTIS-PR-360 available from NTIS at the above address.

DOE/NASA/51040-51
NASA TM-83539

Bending Fatigue of Electron-Beam-Welded Foils

Application to a Hydrodynamic Air Bearing in the Chrysler/DOE Upgraded Automotive Gas Turbine Engine

J. F. Saltsman and G. R. Halford
National Aeronautics and Space Administration
Lewis Research Center
Cleveland, Ohio 44135

January 1984

Work performed for
U.S. DEPARTMENT OF ENERGY
Conservation and Renewable Energy
Office of Vehicle and Engine R&D
Washington, D.C. 20545
Under Interagency Agreement DE-AI01-77CS51040

BENDING FATIGUE OF ELECTRON-BEAM-WELDED FOILS

Application to a Hydrodynamic Air Bearing in the Chrysler/DOE Upgraded Automotive Gas Turbine Engine

by J. F. Saltsman and G. R. Halford

National Aeronautics and Space Administration
Lewis Research Center
Cleveland, Ohio 44135

SUMMARY

A hydrodynamic air bearing with a compliant surface is used in the gas generator of the Chrysler/DOE upgraded automotive gas turbine engine. In the prototype bearing, the compliant surface was a thin foil of Inconel alloy X-750 spot welded to the bearing cartridge, and the foil often failed by fatigue cracking along the line of spot welds. Efforts were initiated to resolve the problem by considering alternate fabrication processes and materials. The alternate fabrication process chosen was electron beam welding rather than spot welding, and Inconel alloy 718 was selected as an alternate material. The alloy X-750 was tested in both the as-welded and welded plus heat treated conditions, while alloy 718 was tested only in the welded plus heat treated condition.

Room temperature bending fatigue results indicated that there is little apparent difference in the total fatigue lives of the welded foil materials tested. Alloy X-750, as-welded, did appear to exhibit a lower crack initiation life, but longer crack propagation life than either alloy X-750 or alloy 718 in the welded plus heat treated condition. However, there is considerable scatter in the data, so it is difficult to draw firm conclusions from the results of the tests. The quality of the welds would have to be improved considerably if electron beam welding were to become a viable option to spot welding for air bearing manufacture. Design options that avoid welding of any kind would appear to offer the greatest potential for increased bearing durability.

INTRODUCTION

A hydrodynamic bearing with an air lubricated compliant surface is used as a journal bearing in the gas generator of the Chrysler/DOE upgraded automotive gas turbine engine. In the prototype bearing, the compliant surface is a thin foil spot welded to a spacer block which is an integral part of the bearing cartridge. The design details of the bearing are given in references 1 to 3, and figure 1 shows the location of the foil bearing in the engine. The gas generator rotor operates in the speed range of 30 000 rpm at idle to nearly 60 000 rpm at full speed and is supported at the hot end by the foil journal air bearing. The normal operating temperature of the foil bearing is 260° C (500° F). A conventional oil-lubricated journal bearing supports the rotor at the cold end. A schematic view of the foil bearing is shown in figures 2 and 3.

The performance of the prototype air bearing was encouraging in that adequate basic air film load capacity was demonstrated under static and dynamic load conditions. However, problems were experienced in three areas, all related to the top foil.

(a) fatigue cracking of the top foil along the line of spot welds
(b) localized heavy burnishing with occasional foil metal transfer to the journal
(c) loss of dry film lubricant coating

In this report, we are concerned only with the fatigue cracking of the top foil.

Alternate fabrication processes and materials were considered in an effort to increase the fatigue life of the top foil. In the prototype bearing, the top foil was spot welded to the spacer block on the bearing cartridge, and the foil failed along the spot welds as shown in figure 3. The alternate fabrication process chosen was electron beam (EB) welding of the top foil to the spacer block. This process offers a higher degree of geometric unformity of the weld.

Inconel alloy X-750 is currently used in the prototype bearing because of its availability, cost, and overall mechanical and physical properties. Inconel alloy 718 was chosen as the alternate material because of its similar excellent characteristics.

The purpose of this investigation was to determine the relative ranking of alloy X-750 and alloy 718 when the foils were EB-welded to the spacer block.

NOMENCLATURE

A	coefficient for plastic strain contribution to nominal total strain range
a	exponent on life for plastic strain contribution to nominal total strain range
B	coefficient for elastic strain contribution to nominal total strain range
b	exponent on life for elastic strain contribution to nominal total strain range
C	correction factor
c	foil half thickness
D	tensile ductility, -ln(100 - RA)/100
E	modulus of elasticity, unprimed-test value; primed-new value
I	moment of inertia of foil cross section
L	moment arm length
M	bending moment
N	number of cycles
P	load at free end of foil
RA	reduction of area in tensile test, percent
S	machine stroke range
t	foil thickness = 2c
w	width of foil
δ	deflection amplitude at loaded end
$\Delta\varepsilon$	nominal total strain range
$\Delta\sigma$	nominal stress range

ν Poisson's ratio
σ stress amplitude

Subscripts:

e elastic
f failure
i initiation
p plastic
T transition

EXPERIMENTAL METHOD

The type of specimen used in this program is shown in figure 4. The 0.102 mm (0.004 in.) thick foil was electron beam (EB) welded to a base of type 310 stainless steel with a 0.279 mm (0.011 in.) spacer block between the foil and the base. This configuration accurately duplicated the design detail of interest of the actual bearing. Justification for using a flat test specimen is given in the ANALYSIS section. The welding parameters and subsequent heat treat specifications are given in tables 1 and 2. Both materials were supplied in the annealed condition. Warpage of the foils following welding was visually evident for all of the specimens (fig. 4(a)).

The bending fatigue test setup is shown in figure 5. Figure 5(a) shows the setup prior to inserting the specimen. Figure 5(b) shows the specimen placed on the locating block, and figure 5(c) shows the specimen clamped in place. Just prior to clamping, the specimen was adjusted so the bending moment arm length was 11.049 mm (0.439 in.). The foil was lightly impinged upon by the round-edged plates on the loading fixture that alternately push up and down on the foil to produced the desired fatigue loading. The stroke of the loading fixture was controlled by an adjustable rotating eccentric.

In conducting the tests, the cycle counter was set for a predetermined number of cycles. At the end of the loading block, the specimen was removed from the machine and examined. If the specimen was cracked, the crack length was measured. The specimen was then put back in the machine for another block of loading. If the specimen failed during a block, one-half of the number of cycles of that block was added to the current cycle count to obtained the number of cycles to failure, N_f. The number of cycles to crack initition, N_i, is the number of cycles the specimen experiences without cracking. The loading block during which the first crack appears is not included in this value. The number of cycles per loading block was estimated based on previous test results. The number of cycles per block at the beginning of a test was kept low. So if a crack developed early, the number of cycles to initiation, N_i, could be determined without undue relative error.

The specimens were tested at room temperature in a displacement (or strain) limited mode. This simulates the type of loading condition experienced by the bearing foil during actual operation. Testing frequency was adjusted to suit each particular test. As noted earlier, the gas generator rotor operates at 30 000 to 60 000 rpm. Thus the bearing foil is excited at 30 000 to 60 000 cpm assuming one cycle per revolution. The maximum operating frequency the fatigue machine is 5000 cpm, but the tests were conducted at much

lower frequencies to prevent fretting of the foil where it was contacted by the round-edged plates. The disparity between operating and testing frequency should be of no concequence, however, because the fatigue behaviour of the alloys is insensitive to frequency effects for both the test and operating conditions.

ANALYSIS

The top foil, figure 3, experiences cyclic bending, and hence fatigue, where it is welded to the spacer block. Thus it is necessary to perform an analysis in this region to determine the magnitude of the cyclic stress level in this region. The top foil can be considered to be a curved cantilever beam with a very high diameter/thickness ratio of 375. The theory of curved beams (ref. 4) shows that for this high ratio the effects of curvature can be ignored and the foil can be analyzed as a straight member. Because of this, a straight cantilever test specimen can be used to determine the relative ranking of the fatigue strength of the foil materials. The test specimen design is discussed in the EXPERIMENTAL METHOD section.

The nominal stress and deflection of the cantiliver beam fatigue specimens were calculated on an elastic basis using the following equations (see nomenclature list for definition of symbols).

Stress amplitude

$$\sigma = \frac{Mc}{I} \tag{1}$$

Deflection amplitude

$$\delta = \frac{PL^3}{3EI} \tag{2}$$

Since the foil is the wide relative to its thickness, EI is replaced by $EI/(1-\nu^2)$ to account for the Poisson effect.

$$\delta = \frac{PL^3(1-\nu^2)}{3EI} \tag{3}$$

But $M = PL$

Thus

$$\delta = \frac{ML^2(1-\nu^2)}{3EI} \tag{4}$$

or

$$M = \frac{(3EI)(\delta)}{L^2(1-\nu^2)} \tag{5}$$

Substituting equation (5) into equation (1) we obtain

$$\sigma = \frac{1.5Et\delta}{L^2(1 - \upsilon^2)} \tag{6}$$

Thus equation (6) relates nominal stress amplitude in the foil at the welded end to the displacement amplitude at the loaded end of the wide cantilever beam.

Equation (6) can be converted to stress range by multiplying both sides by 2. Displacement amplitude at the free end of the foil is replaced by one-half of the total machine stroke, S.

$$\Delta\sigma = \frac{1.5ESt}{L^2(1 - \upsilon^2)} \tag{7}$$

For the test specimens used herein, the appropriate values for the foil thickness, t, moment arm, L, and Poisson's ratio, υ, are:

$$t = 0.102 \text{ mm}$$

$$L = 11.049 \text{ mm}$$

$$\upsilon = 0.30$$

Using these values, equation (7) becomes,

$$\Delta\sigma = 0.00137(E)(S) \tag{8}$$

where the stroke, S, is expressed in millimeters.

Equation (8) can be converted to nominal strain range (percent) by dividing by the modulus of elasticity, E, and mulitplying by 100.

$$\Delta\varepsilon = 0.137(S) \tag{9}$$

This equation determines the nominal total strain range, calculated on an elastic basis, for a given fatigue machine stroke.

RESULTS AND DISCUSSION

The results of the fatigue tests are listed in table 3. The nominal stress range and nominal total strain range were calculated using equations (8), and (9), respectively. Nominal total strain range vs. cycles to failure, N_f, data are plotted in figure 6 along with two equations of the following form (see Appendix A).

$$\Delta\varepsilon = A(N_f)^{-0.60} + B(N_f)^{-0.12} \tag{10}$$

The upper curve in figure 6 is a best-fit of the dataset and is given by the following equation.

$$\Delta\varepsilon = 140(N_f)^{-0.60} + 0.56(N_f)^{-0.12} \tag{11}$$

The total strain range at the transition point (were the two terms in eq. (11) are equal) is 0.28 percent, and the transition fatigue life, N_T, is 100 000 cycles.

The lower dotted line in figure 6 is a "minimum" life line and was obtained by shifting the best-fit line horizontally to the left so every data point is either on or to the right of the line. The equation for this minimum life line is:

$$\Delta\varepsilon = 79.2(N_f)^{-0.60} + 0.43(N_f)^{-0.12} \qquad (12)$$

The total strain range at the transition point is still 0.28 percent, and the corresponding "minimum" transition life is 12 000 cycles, i.e., the minimum curve has been reduced by more than a factor of 8 in life from the average. The large scatter in the data is quite evident and is attributed to the poor quality of the welds.

For most specimens, the foils were warped and the weld beads were rough and irregular. In some cases there was local burn-thru of the foil. Most of the warping occured during welding with some additional warping during heat treat. Program constraints, unfortunately, did not permit experimentation with the welding parameters to improve weld quality. Additional efforts must be made to improve the quality of the welds if EB welding is to be a viable option for manufacturing air foil bearings.

The ability of equation (11) to represent the data is shown in figure 7. In this figure, fatigue data for each alloy is plotted separately for clarity. Here calculated life is plotted vs. observed life. The central line in figure 7 represents exact agreement between observed and calculated life. The lines above and below the central line represent factors of 2 variation between predicted and observed lives. Inset in each figure is a table summarizing a measure of the accuracy of the calculations. The calculated life can be obtained by a trial-and-error solution of equation (11) until the calculated strain range agrees with the nominal strain range of the test, or a direct solution can be obtained by using the inversion method of Manson and Muralidharan (5).

An estimate of how much the fatigue strength of the foil materials is degraded by welding can be obtained from examining the fatigue data for alloy X-750 sheet (ref. 6, fig. 42). The thickness of the sheet is unknown but very likely greater than the 0.102 mm (0.004 in.) foil used in the tests reported herein. The data from reference 6 are plotted in figure 8 along with the best-fit curve.

$$\Delta\varepsilon = 330(N_f)^{-0.60} + 1.32(N_f)^{-0.12} \qquad (13)$$

The transition life is 100 000 cycles, the same as for the welded foil, and the corresponding total strain range is 0.66 percent. The nominal fatigue curve for the EB welded foil (eq. (11)) is shown for comparison.

Since the transition lives (and the exponents, -0.60 and -0.12) for the sheet and welded foil are the same, the two life curves, equation's (11) and

(13) are vertically displaced by a constant amount. This displacement is given by the ratio of the transition strains, or 2.36. Thus to achieve an approximation to the fatigue curve for the welded foil, the fatigue curve for the unwelded sheet can be reduced by a factor (2.36 in this case) to account for the reduction in fatigue strength due to EB welding. This procedure is analagous to applying a strain concentration factor to the smooth sheet fatigue curve to ascertain the welded (notched) behavior.

Nominal total strain range vs. cycles to crack initiation, N_i, are plotted in figure 9. These data suggest that alloys X-750 and 718 in the welded plus heat treated condition have similar crack initiation lives, and alloy X-750, as-welded, has a lower crack initiation life. As noted in the EXPERIMENTAL METHOD section, the test specimen configuration accurately duplicates the design detail of interest in the actual bearing. Thus the initiation behavior noted here should also occur in the actual bearing. A best-fit was done for these data with the transition strain range assumed to be the same as for the failure data (0.28 percent total strain range). The equations for these two sets of data based on crack initiation life (in cycles) are given below.

Alloy X-750, as-welded

$$\Delta\varepsilon = 37.2(N_i)^{-0.60} + 0.43(N_i)^{-0.12} \qquad (14)$$

The transition initiation life is 11 000 cycles.

Alloys X-750 and 718, welded and heat treated

$$\Delta\varepsilon = 68(N_i)^{-0.60} + 0.48(N_i)^{-0.12} \qquad (15)$$

The transition initiation life is 30 000 cycles.

The ability of equations 14 and 15 to represent these data is shown in figure 10. These equations represent the trend of the data fairly well but show more scatter than the failure data (fig. 7).

The current fatigue tests were conducted at room temperature, but the foils operate at 260° C (500° F). Thus it is necessary to be able to estimate the effect of the higher temperature on cyclic life. For this purpose, a useful concept can be discussed with the aid of figure 12 and the universal slopes equation (eq. A-5) in Appendix A. From figure 12, it is apparent that the total strain range line approaches the plastic line for very low cyclic lives and approaches the elastic line for very high cyclic lives. Referring to the universal slopes equation we see that ductility, as measured by the reduction of area, becomes the dominant property for very low cyclic lives and the ultimate tensile strength becomes the dominant property in the very high cycle region.

The life of the bearing must necessarily be in the very high cycle region where ductility effects are very small. Thus the first term on the right hand side of the universal slopes equation, or equation (A-6), involving ductility

can be neglected; and equation (11), for example, can be written in the following form.

$$\Delta\varepsilon = 0.56 \left[\frac{\sigma'_{u/E'}}{\sigma_{u/E}}\right] (N_f)^{-0.12} \tag{16}$$

where the unprimed terms are room temperature values for the specimens tested and the primed terms are for property changes due to changes in alloy, heat treatment or temperature. Thus with equation (16), it is possible to estimate the effects on cyclic life in the high cycle regime due to changes in mechanical properties. Solving equation (16) for N_f.

$$N_f = 7.99\text{x}10^{-3} \left[\frac{\sigma'_{u/E'}}{\sigma_{u/E}}\right]^{8.33} (\Delta\varepsilon)^{-8.33} \tag{17}$$

The terms in the brackets adjust the calculation to account for changes in the ultimate tensile strength and modulus of elasticity with temperature.

$$\text{let} \quad C = \left[\frac{\sigma'_{u/E}}{\sigma_{u/E}}\right]^{8.33} \tag{18}$$

Thus equation (17) can now be written as follows:

$$N_f = 7.99\text{x}10^{-3} (C)(\Delta\varepsilon)^{-8.33} \tag{19}$$

In adjusting the room temperature fatigue results to account for the change in properties due to the change in temperature, we shall use the properties of heat treated alloy X-750 at room temperature and 260° C (500° F) (refs. 6 and 7).

Alloy X-750, Heat Treated

Temperature		Ultimate strength		Modulus of elasticity x10^3	
°C	°F	mpa	ksi	mpa	ksi
21	70	1220	177	213.7	31.0
260	500	1124	163	200.6	29.1

Thus $$C = \left[\frac{1124/200.6}{1220/213.7}\right]^{8.33} = 0.85$$

Thus the fatigue life of the foil at 260° C (500° F) is only reduced to 85 percent of the life at room temperature for the same total strain range. This correction (15 percent) is quite small relative to the scatter in the test data. An appreciation of the amount of scatter present can be gained

from examining the data for the tests conducted at a total strain range of 0.111 percent (table 3, specimen numbers A-4, B-2, and C-2). The observed N_f values range from 1.02 to 14.27 million cycles - a ratio of about 14 to 1. We conclude that the temperature effect is a very small one in the present case. Thus, testing at room temperature is an entirely reasonable approximation to the 260° C (500° F) operating condition. Note that the temperature correction of 0.85 applies only in the high cycle regime where the inelastic term in equation (A-6) can be ignored.

CONCLUDING REMARKS

Room temperature tests were performed using electron beam welded flat foil specimens. The foil materials were Inconel alloy X-750 and Inconel alloy 718. Alloy X-750 was tested in both the as-welded and welded plus heat treated condition, and alloy 718 was tested only in the welded plus heat treated condition. The nominal stress range and strain range in the foil at the weld were calculated using conventional elastic beam theory. The top foil is considered to be a curved cantilever beam with a very high diameter/thickness ratio. And because of this very high ratio, the effects of curvature can be ignored; and the foil can be analyzed as a straight member.

Three curves and corresponding equations are presented to characterize the room temperature fatigue behavior of the foil specimens.

(a) nominal strain range vs. cycles to fracture
(b) nominal strain range vs. minimum cycles to fracture
(c) nominal strain range vs. cycles to crack initiation

(1) The data generated indicates that there is little apparent difference in the total fatigue life characteristics of the foil materials tested. However, alloy X-750, as-welded, apparently has a lower crack initiation life than either alloy X-750 or alloy 718 in the welded plus heat treated conditions. There is considerable scatter in the data, however, so it is difficult to draw firm conclusions from the results of the tests.

(2) An estimate of how much the fatigue resistance of the foil is degraded by welding is obtained from literature data for alloy X-750 sheet. It was found that the nominal strain range-cycles to failure curve for the foil and the alloy X-750 sheet have essentially the same transition life. However, the transition strains are different with the life curve for the welded foil (with concentration factors due to welding) lying below the curve for the sheet by a factor of 2.36.

(3) An equation is presented to estimate the effects on fatigue life due to changes in foil strength due to temperature. The reduction in fatigue life due to increasing the temperature from room temperature to the operating temperature of 260° C (500° F) was estimated to be only 15 percent.

The quality of the welds was not good and undoubtedly contributed to the scatter in the data. The weld beads generally were rough and irregular. In some cases the weld imperfections were sites of crack initiation. At foil edges often there was local burn-through of the foil which was the origin of cracking. Program constraints did not permit experimentation with the welding

parameters to improve weld quality. However, the quality of the welds must be improved considerably if electron beam welding is to be a viable option to the method of spot welding. Design options that avoid welding of any kind would appear to be advantageous and might well provide better fatigue resistance of hydrodynamic foil air bearings.

APPENDIX A

The stress-strain behavior of a material in a fully reversed fatigue cycle is shown in figure 11, where the total strain range is the sum of the plastic and elastic strain ranges.

$$\Delta\varepsilon = \Delta\varepsilon_p + \Delta\varepsilon_e \tag{A-1}$$

For fully reversed, strain controlled fatigue cycling, the relation between total strain range and cyclic life can be expressed in the following form (see fig. 12).

$$\Delta\varepsilon = A(N)^{-a} + B(N)^{-b} \tag{A-2}$$

where

$$\Delta\varepsilon_p = A(N)^{-a} \tag{A-3}$$

$$\Delta\varepsilon_e = B(N)^{-b} \tag{A-4}$$

where A, B, a, and b are material constants obtained from fatigue tests. A schematic plot of this equation is shown in figure 12. The transition point, T, is the point where the plastic and elastic lines intersect.

In conventional push-pull fatigue tests, the plastic and elastic strain ranges can be determined from the hysteresis loop and the fatigue constants can be determined by curve fitting equations (A-3) and (A-4) to experimental data. In bending fatigue tests, the plastic and elastic strain ranges cannot be determined explicitly. Only a nominal total strain range value can be determined using elastic based equations. Thus in the analysis of the present bending fatigue results a less rigorous had to be used to relate total strain range to cyclic life.

A widely used method for estimating fatigue life when suitable material constants obtained from cyclic tests are not available is the universal slopes equation (ref. 8).

$$\Delta\varepsilon = D^{0.60}(N_f)^{-0.60} + \frac{3.5\sigma_u}{E}(N_f)^{-0.12} \tag{A-5}$$

This equation was obtained from an analysis of axial push-pull fatigue data for a large number of materials and the constants represent average values. This equation is quite useful in providing estimates of the cyclic strain resistance of materials, but obviously could never possess the accuracy of cyclic data.

In analyzing the current bending fatigue data, the concept of the universal slopes equation was used since the plastic and elastic strain range values were not directly attainable. Using the exponent values from the universal slopes equation, equation (A-2) becomes

$$\Delta\varepsilon = A(N_f)^{-0.60} + B(N_f)^{-0.12} \qquad \text{(A-6)}$$

The values of A and B were then obtained by a best-fit of the data. By relating equation (A-2) to the universal slopes equation (A-5), it is possible to estimate the effects on cyclic life of changes in mechanical properties. Thus in equation (A-6), changes in ductility will cause a change in A, and changes in ultimate tensile strength or modulus of elasticity will cause changes in the value of B. An example of this is given in the RESULTS AND DISCUSSION section.

REFERENCES

1. Ruscitto, D; McCormick, J.; and Gray, S.: Hydrodynamic Air Lubricated Compliant Surface Bearing For an Automotive Gas Turbine Engine. I: Journal Bearing Performance. (CONS/9427-1, Mechanical Technology; NAS3-19427.) NASA CR-135368, 1978.

2. Gray, S.: Development of Compliant Foil Bearings for Automotive Gas Turbines. Highway Vehicle Systems Contractors Meeting. (CONF-7805102-(Summ.), 1978, pp. 92-111.

3. Gray, S.: Foil Type Bearings for the Chrysler Automotive Gas Turbine Engine Program-Development and Operational Experiences. SAE Paper 790109, Feb. 1979.

4. Roark, Raymond J.: Formulas for Stress and Strain. Fifth ed. McGraw-Hill, 1975, pp. 209-210.

5. Manson, S. S.; and Muralidharan, U.: A Single-Expression Formula for Inverting Strain-Life and Stress-Strain Relations. NASA CR-165347, 1981.

6. Engineering Properties of Inconel Alloy X-750. Technical Bulletin T-38, International Nickel Co., Inc., 1963.

7. INCONEL Alloy X-750. International Nickel Co., Inc., 1970.

8. Manson, S. S.: Fatigue - A Complex Subject-Some Simple Approximations. Exp. Mech., vol. 5, no. 7, July 1965, pp. 193-226.

TABLE 1. - ELECTRON BEAM WELDING SPECIFICATIONS

80 kilovolts, 1.5 milliamps
Speed = 89 cm/min (35 in./min)
Vacuum = 5×10^{4} torr
Performed on 6 kW Hamilton electron beam welder

TABLE 2. - HEAT TREATMENT OF FOILS AFTER WELDING

Inconel alloy X-750
732° C (1350° F) for 20 hr, furnace cool to room temperature
Inconel alloy 718
732° C (1350° F) for 20 hr, 621° C (1150° F) for 10 hr, furnace cool to room temperature

TABLE 3. - TEST RESULTS

(a) Alloy X-750, as-welded

Spec. no.	Stroke		Total strain range-	Stress range[a]		N_i	N_f
	mm	in.		mpa	ksi		
A-2	2.134	0.084	0.292	624.0	90.5	5 000	23 000
A-7	2.134	.084	.292	624.0	90.5	10 000	100 000
A-6	1.448	.057	.198	423.4	61.4	220 000	470 000
A-3	1.067	.042	.146	312.3	45.3	100 000	740 000
A-4	.813	.032	.111	237.2	34.4	6 000 000	14 270 000
A-1	.635	.025	.087	186.2	27.0	----------	4 000 000
A-5	.457	.018	.063	134.5	19.5	1 000 000	17 150 000
$E = 213.7 \times 10^3$ mpa (31.0×10^6 psi)							

(b) Alloy X-750, welded plus heat treated

Spec. no.	Stroke		Total strain range-	Stress range[a]		N_i	N_f
	mm	in.		mpa	ksi		
B-5	2.134	0.084	0.292	624.0	90.5	40 000	70 800
B-7	2.057	.081	.282	602.6	87.4	15 600	55 600
B-3	1.448	.057	.198	423.4	61.4	200 000	575 000
B-1	1.041	.041	.143	305.4	44.3	50 000	424 000
B-2	.813	.032	.111	237.2	34.4	1 700 000	4 100 000
B-4	.635	.025	.087	186.2	27.0	8 000 000	8 330 000
B-8	.483	.019	.066	141.4	20.5	26 400 000	52 000 000
$E = 213.7 \times 10^3$ mpa (31.0×10^6 psi)							

(c) Alloy 718, welded plus heat treated

Spec. no.	Stroke		Total strain range-	Stress range[a]		N_i	N_f
	mm	in.		mpa	ksi		
C-8	2.134	0.084	0.292	584.0	84.7	30 000	341 000
C-6	1.448	.057	.198	395.8	57.4	300 000	1 500 000
C-4	1.067	.042	.146	291.7	42.3	100 000	1 600 000
C-2	.813	.032	.111	222.0	32.2	250 000	1 020 000
C-7	.635	.025	.087	173.8	25.2	500 000	1 480 000
C-1	.483	.019	.066	131.7	19.1	5 000 000	DNF[b]
$E = 200.0 \times 10^3$ mpa (29.0×10^6 psi)							

[a]Elastically calculated.
[b]DNF - did not fail.

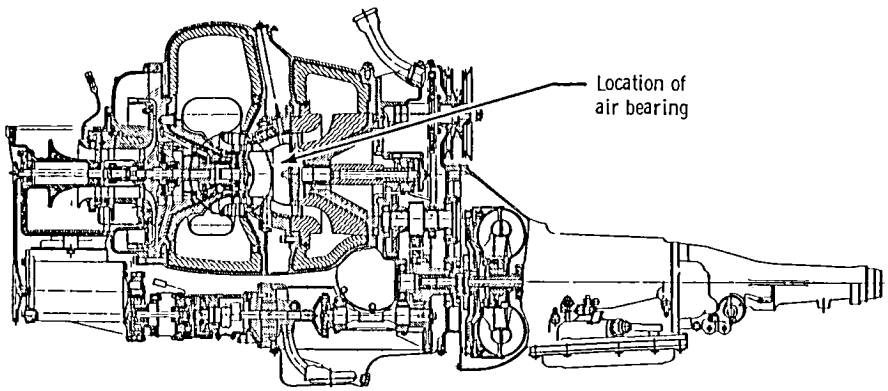

Figure 1. - Chrysler automotive gas turbine with hydrodynamic foil air bearing.

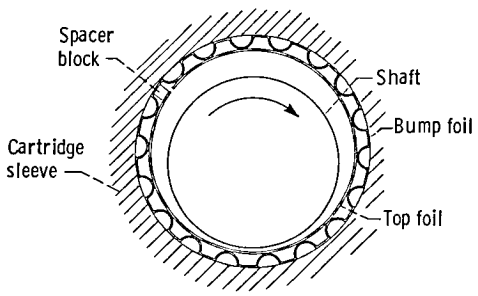

(a) Bearing configuration.

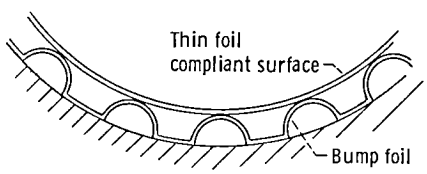

(b) Cross section of bearing.

Figure 2. - Schematic of hydrodynamic compliant surface journal bearing.

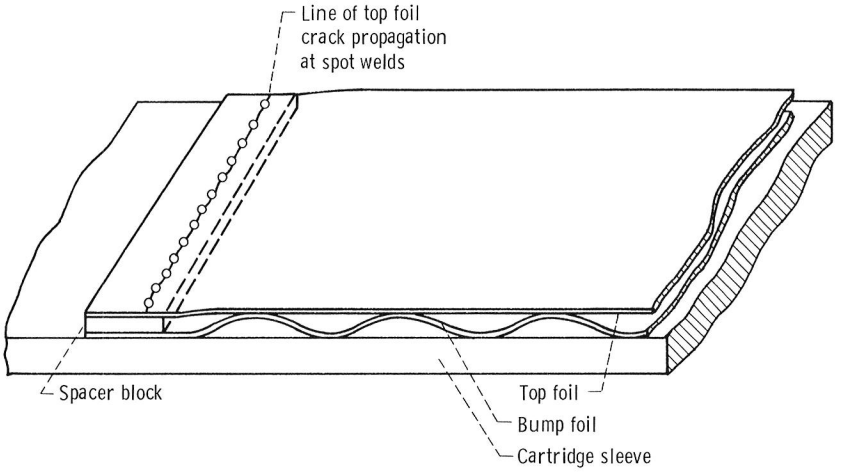

Figure 3. - Unwrapped view of air bearing.

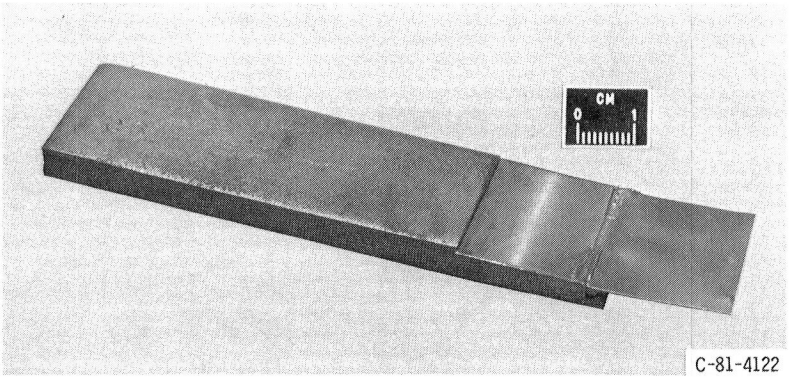

(a) As fabricated

Figure 4. - Fatigue specimen. (Dimensions in millimeters (inches).

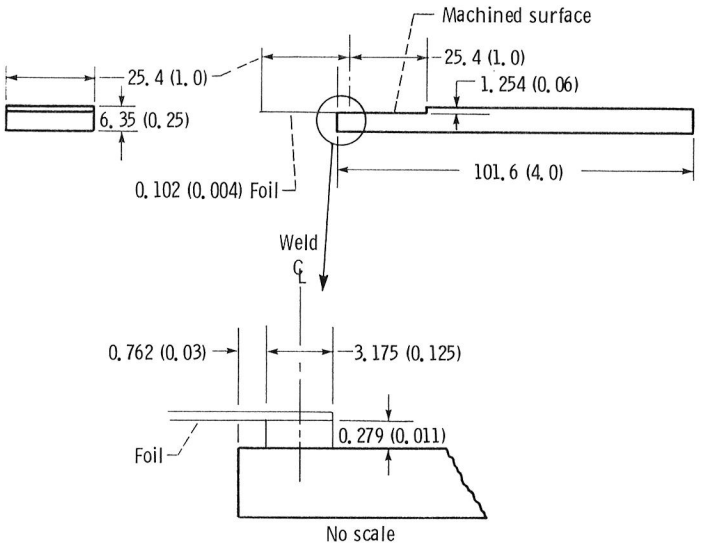

(b) Specimen dimensions.

Figure 4. - Concluded.

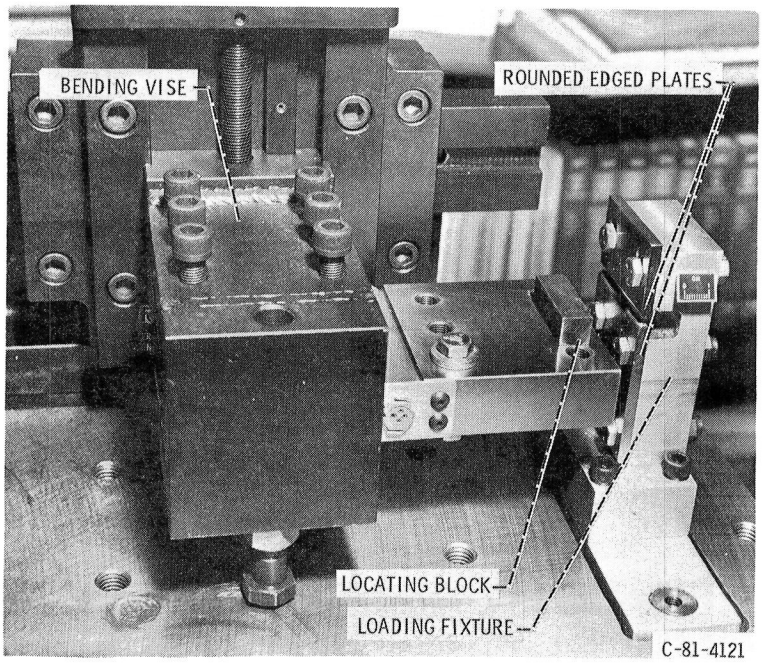

(a) Test setup pior to inserting specimen.

Figure 5. - Specimen bending vise and loading fixture.

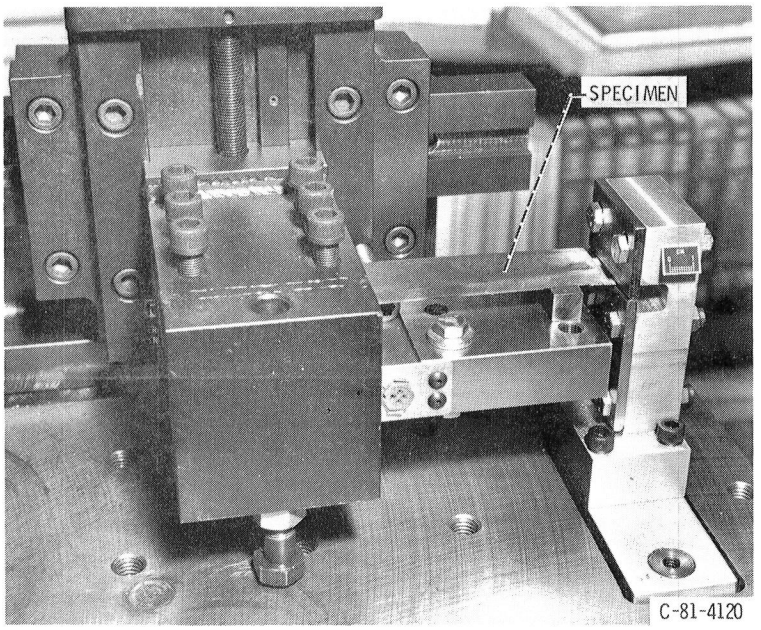

(b) Specimen placed on locating block.

Figure 5. - Continued.

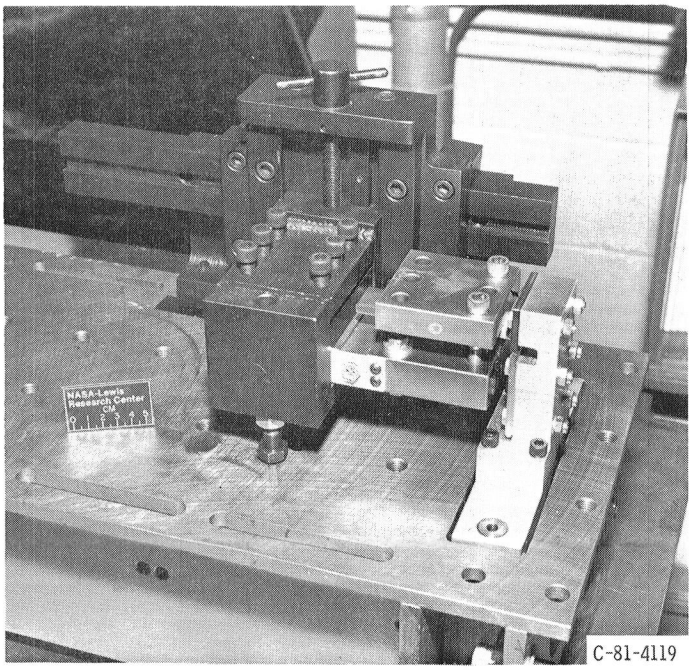

(c) Specimen clamped in place.

Figure 5. - Concluded.

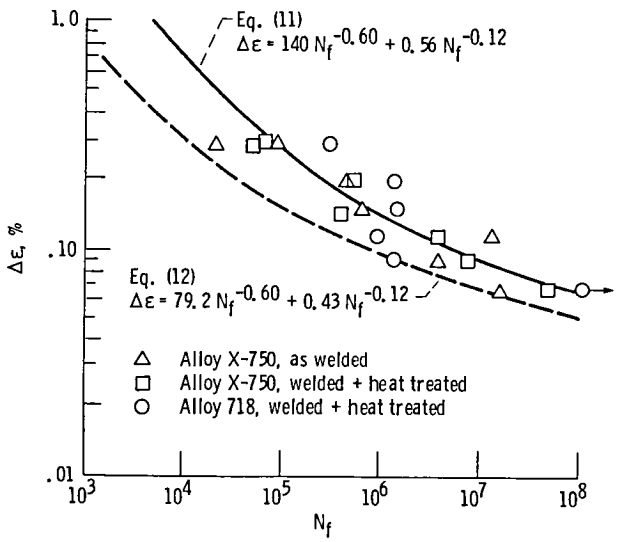

Figure 6. - Nominal strain range versus cycles to failure.

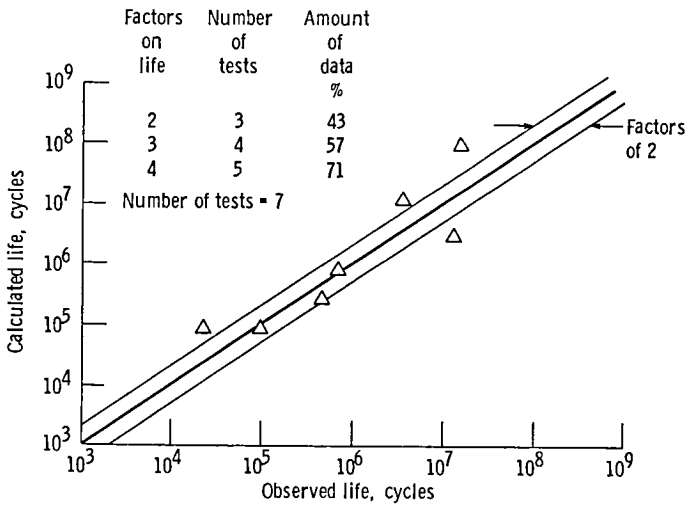

(a) Alloy X-750, as-welded.

Figure 7. - Life calculation of fatigue data using eq. (11).

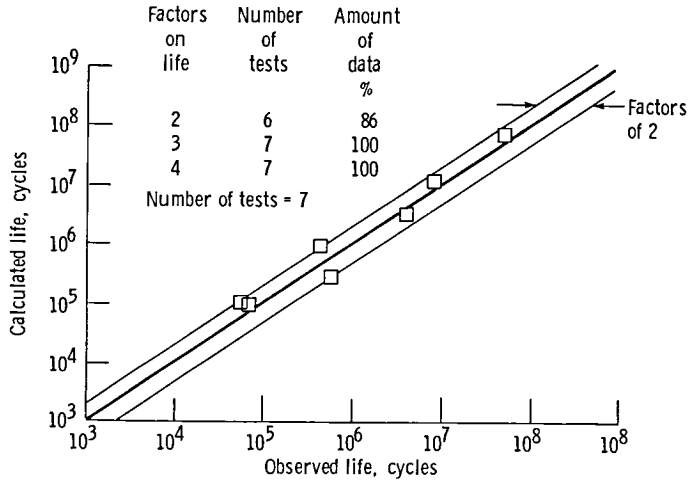

(b) Alloy X-750, welded plus heat treated.

Figure 7. - Continued.

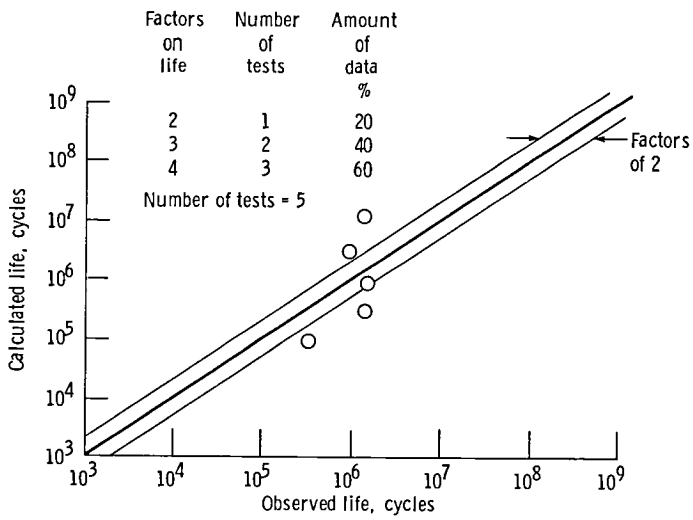

(c) Alloy 718, welded plus heat treated.

Figure 7. - Concluded.

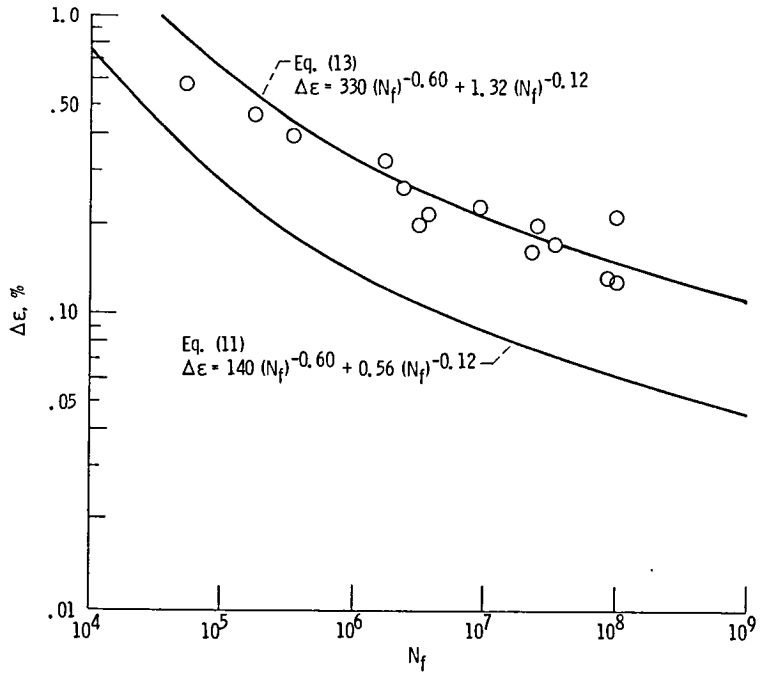

Figure 8. - Nominal strain range versus cycles to failure for alloy X-750 sheet. (Ref. 6.)

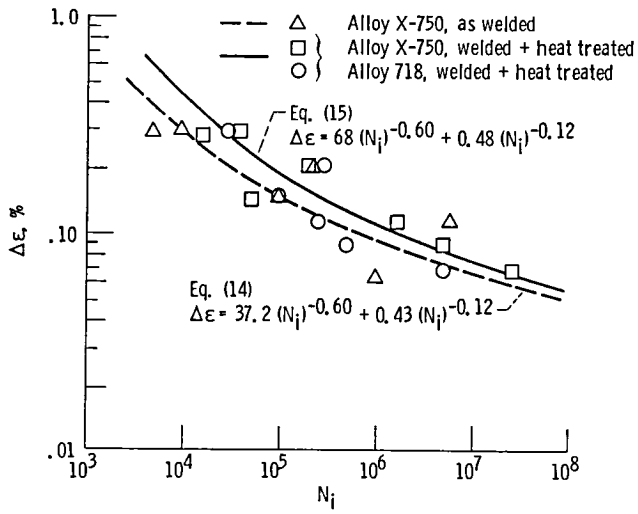

Figure 9. - Nominal strain range versus cycles to crack initiation.

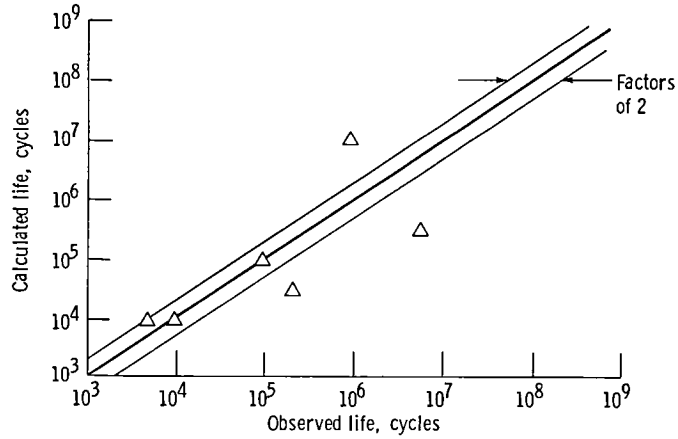

(a) Alloy X-750, as welded - Eq. (14).

Figure 10. - Calculation of cycles to crack initiation.

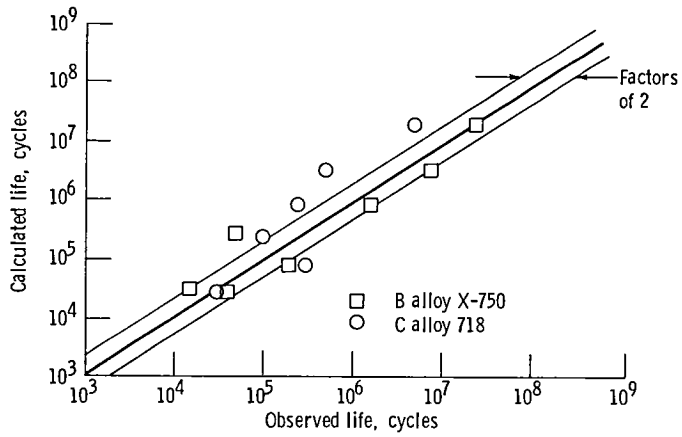

(b) Alloy X-750 and alloy 718 welded plus heat treated - Eq. (15).

Figure 10. - Concluded.

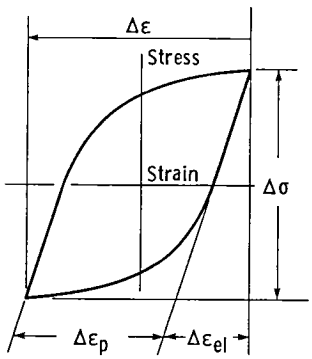

Figure 11. - Hysteresis loop.

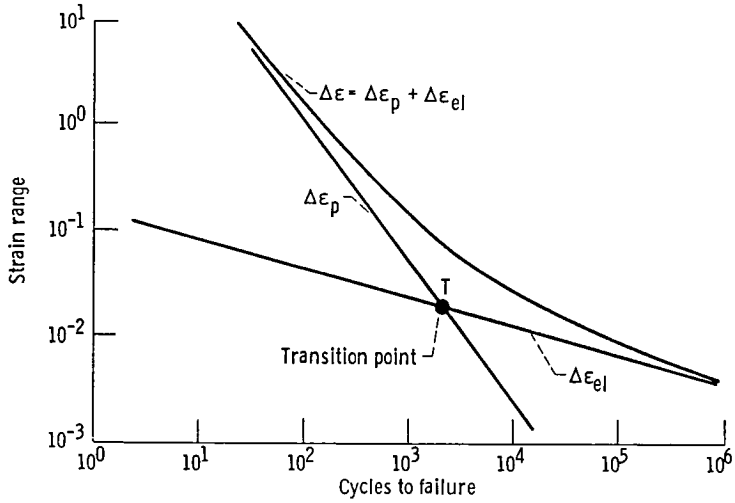

Figure 12. - Schematic of total strain range versus cycles to failure.

1. Report No.	2. Government Accession No.	3. Recipient's Catalog No.
NASA TM-83539		

4. Title and Subtitle	5. Report Date
Bending Fatigue of Electron-Beam-Welded Foils Application to a Hydrodynamic Air Bearing in the Chrysler/DOE Upgraded Automotive Gas Turbine Engine	January 1984
	6. Performing Organization Code 778-32-001
7. Author(s) J. F. Saltsman and G. R. Halford	8. Performing Organization Report No. E-1910
	10. Work Unit No.
9. Performing Organization Name and Address National Aeronautics and Space Administration Lewis Research Center Cleveland, Ohio 44135	11. Contract or Grant No.
	13. Type of Report and Period Covered Technical Memorandum
12. Sponsoring Agency Name and Address U.S. Department of Energy Office of Vehicle and Engine R&D Washington, D.C. 20545	14. Sponsoring Agency ~~Code~~ Report No. DOE/NASA/51040-51

15. Supplementary Notes

Final report. Prepared under Interagency Agreement DE-AI01-77CS51040.

16. Abstract

A hydrodynamic air bearing with a compliant surface is used in the gas generator of the Chrysler/DOE upgraded automotive gas turbine engine. In the prototype design, the compliant surface is a thin foil spot welded at one end to the bearing cartridge. During operation, the foil failed along the line of spot welds which acted as a series of stress concentrators. Because of its higher degree of geometric uniformity, electron beam welding of the foil was selected as an alternative to spot welding. Room temperature bending fatigue tests were conducted to determine the fatigue resistance of the electron beam welded foils. Equations were determined relating cycles to crack initiation and cycles to failure to nominal total strain range. A scaling procedure is presented for estimating the reduction in cyclic life when the foil is at its normal operating temperature of 260° C (500° F).

17. Key Words (Suggested by Author(s))	18. Distribution Statement
Bending fatigue; Fatigue life; Welded joints; Temperature effects; Air bearings; Nickel alloys	Unclassified - unlimited STAR Category 39 DOE Category UC-96

19. Security Classif. (of this report)	20. Security Classif. (of this page)	21. No. of pages	22. Price*
Unclassified	Unclassified	18	A02

*For sale by the National Technical Information Service, Springfield, Virginia 22161